

## 1D VS 3D STRONG GROUND MOTION HYBRID MODELLING OF SITE, AND PRONOUNCED TOPOGRAPHY EFFECTS AT AUGUSTA RAURICA, SWITZERLAND - EARTHQUAKES OR BATTLES?

Ivo OPRISAL<sup>1</sup>, Donat FÄH<sup>2</sup>

### ABSTRACT

Numerical modelling using 1D and 3D techniques has been applied to the Roman city of Augusta Raurica, located East of Basel, Switzerland. One important topic of the city's history concerns the hypothesis of an earthquake striking the city in the middle of the third century A.D. The 3D finite-difference (FD) method computes the full 3D wave field by a hybrid approach on an irregular grid. Topography is included in the modelling. The 1D-matrix method is used to model the P-SV response for 195 x 213 1D structures extracted from the 3D computational model by retrieving a vertical profile under each surface point. The incoming wave field is realized by a vertically incident planar wave for a family of sources. The established three-dimensional velocity structure for the studied area comprises (as geophysical bedrock) a limestones unit (Muschelkalk), tertiary sediments (Keuper), and Quaternary gravel layers. The area is characterized by a pronounced topography. The soft-sediment cover is typically not thicker than 50m. Pseudo-spectral response amplification (PSAA, 5%-damping) for frequencies between 0.1Hz and 10Hz shows values up to factor 4.6 in the 1D case and up to factor 9.1 in the 3D computations. The locations of the largest amplifications differ between the 1D and 3D method. Thus the 3D - vs.1D- amplification is expressed by a ratio of about 2.5, usually at the top of the most pronounced topographic features within the Quaternary formation.

Keywords: finite difference, hybrid modelling, site effects, spectral amplification, topography

### INTRODUCTION

Earthquake ground motion modelling is complementary to the archaeological and geological investigations made in Augusta Raurica archaeological site the suburbs of the Basel City, Switzerland. The 1D approximation to the topmost structure, in terms of fundamental frequencies, allows for refinement of the upper geology and the shape of the interface limiting it from below. Array investigations are sensitive to bedrock structures. Therefore it is advisable to test the dependence of PSAA valued on the bedrock models of the 3D wave field propagation methods.

PSAA is a good means to investigate the site effects because it's nature and sensitivity are close to real constructions. Moreover classical approach of PGA imaging is generally blind at spots of prolonged lower-amplitude shaking. The hypothesis of an 250 AD earthquake striking the city ( resulting in anomalous destruction of the walls and unusual way of positioning the buried bodies can be tested by the 3D wave propagation methods like finite differences. Including extended source of a close earthquake in the hybrid FD approach accounts for a more realistic scenario.

---

<sup>1</sup> PhD., Faculty of Mathematics and Physics, Charles University in Prague, Czech Republic, Email: [io@karel.troja.mff.cuni.cz](mailto:io@karel.troja.mff.cuni.cz), Now at DPRI - Disaster Prevention Research Institute, Kyoto, Japan

<sup>2</sup> PhD., Swiss Seismological Service, Swiss Federal Institute of Technology – ETH, Zurich, Email: [donat.faeh@sed.ethz.ch](mailto:donat.faeh@sed.ethz.ch)

## GEOLOGY

### Refining upper geology model

The geological model as defined by Fäh et al (2006) consists of geophysical bedrock composed of limestones unit (Muschelkalk), tertiary sediments (Keuper), and Quaternary gravel layers, see Figure 1. Approximations and refinement described later use the best available information up-to-date.

These layers are defined by interfaces between their topmost part and above layer, including topography. Top\_ Muschelkalk, Top\_Keuper, and topography are the main interfaces defining the layers, respectively from depth. The sub-structure inside each of these layers is given by vertical 1D profile that always copies the top interface of the actual layer.

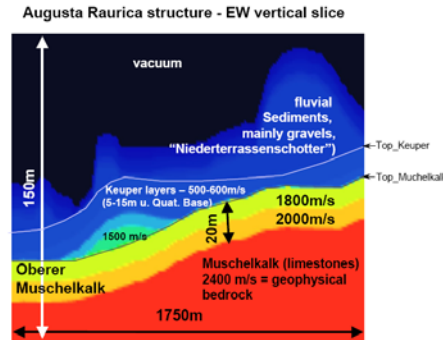


**Figure 1.** Geological model sample for one of the EW vertical slices at Augusta Raurica. This is a 3D FD computational model extraction. See also Figure 4.

The topography was retrieved (by digitization) from topography map (pers. comm. J. Ripperger) and transferred, as well as Top\_ Muschelkalk, and Top\_Keuper layers, to DXF format (Ripperger, 2003). For our needs, the topography was re-sampled into a square-grid 10m horizontal grid step in NS and WE directions and continuous elevation values at these points.

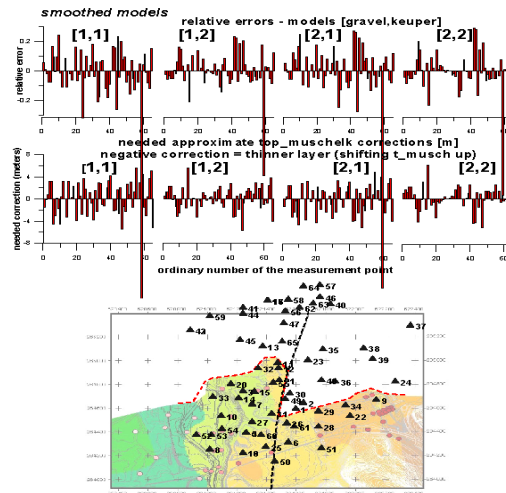


**Figure 2.** Corrections applied to original geological model with respect to measured and computed fundamental frequencies in 60 points (black triangles) of the area. The right panel shows approximate Top\_ Muschelkalk corrections in meters to reach the 0% difference in relative eigen frequencies. The red line on the lower panel depicts the Northernmost outreach of the Keuper layer.

Because the horizontal extent of the interfaces, given by the available information, is mutually differing, we extended the horizontal size of Top\_ Muschelkalk to the size of Top\_Keuper and the topography. The extension is constructed so, that the difference between the topography and Top\_ Muschelkalk is constant from each of the North most defined point of original Top\_ Muschelkalk (red line of Lower panel at Figure 2) in the direction perpendicular to the border defined by such a

point. The corners are extended likewise since the whole section keeps the corner point difference from the free surface.

Apparently (Figure 18 of Ripperger, 2003 – or the lower panel of Figure 2), the thickness of Keuper (lying between Top\_Keuper and Top\_muschelkalk) is considered non-zero before reaching the ~264.5 km North and equal to zero above ~265.05 km North (Swiss system). The available interface data do not satisfy this condition. As a result we tapered the Top\_Keuper thickness from the value (given by interfaces) to zero by 50 m broad taper according to Figure 18 of Ripperger (2003). The linear taper of 50 m breadth is applied. The horizontal direction of the tapering is 11.5° clockwise from north (for numerical reasons). Finally, a constraint (elevation of topography)  $\geq$  (elevation of Top\_Keuper)  $\geq$  (elevation of Top\_Muschelkalk) is applied.

Each of the fluvial sediments (predominately gravels, Pleistocene, “Niederterrassenschotter”) and Keuper layers (15m upper quaternary and quaternary base) has 2 possible generic modifications (See Fäh et al, 2006, and Table 1). From now on we will indicate the possible combination of these variants in the model as [gravel\_No, Keuper\_No], e. g., model [1,2] means that gravel variant No. 1 and Keuper variant No. 2 is used in the model. The geology described in Table 1 is defined generally and is cropped by the respective upper and lower interfaces defining each layer.

The geology of the topmost part may be approximately verified by comparing the eigen frequency in each surface point (for a vertical profile under such point) with the measured maximum in the H/V ratio measurements. The fundamental frequency corresponds to maximum of H/V ratio  $\sim f_0$  (fundamental mode of Love surface waves with minimum (or none in pure 1D) ground motion in vertical direction). Considering single layer with thickness  $h$  and constant or average (harmonically averaged in vertical direction) shear wave velocity  $V_s$ , the fundamental frequency  $f_0$  is given by a simple formula  $V_s = 4 h f_0$ . We did such a comparison for 64 points and all 4 combinations of [gravel\_No, Keuper\_No] or [gravel, Keuper], denoted as [1,1],[1,2],[2,1],[2,2]; where Top\_Muschelkalk was the main interface. Consequently, the Top\_Muschelkalk interface was shifted to fit its 1D computed eigen frequencies exactly with the measured one in each point. However, the computed correction for the whole Top\_Muschelkalk (and possibly the other layers) had to be strongly smoothed due to the correction values and distribution of the stations. Resulting difference between needed and finally applied smoothed changes are given (for each measurement point) in Figure 2. Typical relative errors between computed and measured eigen frequencies for all of [gravel, Keuper] combinations and all measurement points were under 15%, where large-per-cent changes correspond to small (~1m) changes in actual interface position (see Figure 2). After careful analysis of the eigen frequencies (Figure 2) and some additional computations shown below, we decided to take [1,2] as the most favourable [gravel, Keuper] model.

The top 20m of the geophysical bedrock (Muschelkalk) being mainly limestones is topped by 2 x 10 m thick Oberer Muschelkalk composed of Triassic carbonate sequences (see Table 2). All rastered interfaces are available in a form of ASCII GIS file format (e.g., directly readable by 'Arcview spatial analyst'). The Fortran subroutine returning the material parameters in each point given North, East, and elevation coordinates and [gravel,Keuper] combination are available as a part of the output data package.

## Reference models

The reference model is a 1D model with flat-surface surface corresponding to Top\_muschelkalk, and further layers defined. The 3D model with a reference bedrock means that the interfaces and layers of the bedrock starting from Top\_muschelkalk down to 500m in the bedrock structure copy the Top\_muschelkalk interface (see Figure 1).

There are 2 generic modifications to the SWISS ROCK (Fäh, personal communication) model (originally 63 layers): Simpler Swiss 1 and more complex Swiss 2 bedrock. To test the relevancy of

the reference bedrock model, we have applied also bedrock Swiss 2 LO and Swiss 2 Hi modifications of the Swiss 2.

The quality factor is considered  $Q_s=25$  down to 150 m under topmost point of an actual model, then linearly growing from  $Q_s=25$  to  $Q_s=100$  from 150 m down to 650 m, respectively and being equal to 100 for larger depths. For all model details see Table 2.

**Table 1. Top-geology gravel and Keuper models.**

Depth (m)	Density (g/cm <sup>3</sup> )	Vp (km/s)	Qp	Vs (km/s)	Qs	Depth (m)	Density (g/cm <sup>3</sup> )	Vp (km/s)	Qp	Vs (km/s)	Qs
gravel==1						gravel==2					
2	1.8	0.8	30	0.36	15	3	1.8	0.8	30	0.30	15
4	1.8	0.8	50	0.37	25	6	1.8	0.8	50	0.34	25
6	1.8	0.8	50	0.39	25	8	1.85	1.0	50	0.40	25
8	1.85	1.0	50	0.43	25	10	1.85	1.0	50	0.42	25
10	1.85	1.0	50	0.44	25	12	1.85	1.0	50	0.44	25
12	1.85	1.0	50	0.45	25	14	1.85	1.4	50	0.48	25
14	1.85	1.4	50	0.50	25	16	1.85	1.4	50	0.52	25
16	1.85	1.4	50	0.53	25	20	1.85	1.4	50	0.54	25
20	1.85	1.4	50	0.55	25	20+	1.85	1.4	50	0.54	25
20+	1.85	1.4	50	0.55	25						
Keuper==1						Keuper==2					
10	2.00	2.15	50	0.67	25	10	2.00	2.00	50	0.58	25
20	2.15	2.73	50	0.96	25	17	2.00	2.10	50	0.60	25
40	2.30	3.30	50	1.65	25	18	2.00	2.30	50	0.65	25
40+	2.30	3.30	50	1.65	25	24	2.15	2.70	50	0.90	25
						35	2.30	3.10	50	1.25	25
						40	2.30	3.10	50	1.50	25
						40+	2.30	3.10	50	1.50	25

**Table 2: The reference models used for the computations.**

Depth (km)	Density (kg/m <sup>3</sup> )	Vp(km/s)	Vs(km/s)	Depth (km)	Density (kg/m <sup>3</sup> )	Vp(km/s)	Vs(km/s)
Bedrock Swiss 1				Bedrock Swiss 2			
10	2300	3.15	1.8	10	2300	2.4	1.2
20	2400	3.4	1.97	20	2300	2.8	1.4
700	2500	4.2	2.42	30	2300	3.15	1.8
				140	2400	3.2	1.85
				260	2400	3.3	1.91
				380	2400	3.4	1.97
				500	2400	3.8	2.19
				700	2500	4.2	2.42
Bedrock Swiss 2 LO				Bedrock Swiss 2 HI			
10	2300	2.4	1.2	10	2300	2.4	1.2
20	2300	2.8	1.4	20	2300	2.8	1.4
30	2300	3.15	1.8	30	2300	3.15	1.8
140	2400	3.2	1.85	140	2400	3.2	1.85
260	2400	3.3	1.91	260	2400	3.3	1.91
380	2400	3.4	1.97	380	2400	3.4	1.97
500	2400	3.8	2.19	500	2400	3.8	2.19
700	2450	3.45	2.0	700	2650	4.85	2.8

## COMPUTATIONAL METHODS

### Pseudo Spectral response and amplification

The behaviour of the wave field propagating through a particular model is investigated by means of 'pseudospectral acceleration' PSA, computed as 5%-damping spectral velocity response for both horizontal components. For our needs

$$PSA(\omega) = \omega^2 SD(\omega), \quad (1)$$

where SD are the computed spectral response displacement maxima in time domain. The SD is computed by a 2-component standard time-marching finite-difference template, with surface ground motion acceleration as input. Finally,  $\omega$  is angular frequency corresponding to a particular SD value, thus 'pseudo spectral acceleration'.

The PSA amplification (PSAA) defined as  $PSA(model)/PSA(reference)$  for all surface points covering the 1552 m (WE) x 1696 m (SN) large rectangular area with equal horizontal distance between the points being 8 m (195 x 213 points). The SW corner of the investigated area being at [620800North,264055East] (meters of the SWISS COORDINATE SYSTEM). This applies also for all the panels and sub-panels introduced in this paper.

### Wave field modelling

The wave field, resulting in surface ground motion as an input for the PSA analysis, is computed by 2 methods:

1. Hybrid 3D finite-difference (FD) modelling on irregular grids (Opršal and Zahradník, 2002, Opršal et al., 2002; 2004; 2005) computes the full 3D wave field by hybrid injection of the wave field. Here, the 3D wave field is injected by prescribing vertically incident planar wave at the hybrid procedure boundary. The structure with topography is approximation of 3D geology to a computational model (Opršal and Zahradník, 2002, par. 2.5). A simplified employment of wave propagation attenuated in anelastic media is approximated by  $Q_p=Q_s=Q(x,y,z)=c*f$  where  $f$  is the prevailing frequency of the signal, here  $f=5\text{Hz}$  (Zahradník et al., 1990a, 1990b, Graves 1996, Opršal et al, 2005, par. 3.3). The structure is 3D geological approximation transformed to a computational model. We compute for frequencies 0-12Hz with usable range 0-10Hz.

2. 1D-pseudo-3D modelling "locally 1D": Under each of the above defined surface points we had extracted individual 1D structure from the 3D FD computational model by retrieving a vertical profile under each such point. Then the 1D structure generally differs from point to point and therefore the 1D computation is performed separately for every individual structure. Matrix method for 1D layered media of (Mueller, 1985) is used to compute the 1D P-SV response for the respective S-wave. The code was adopted after Bartak and Zahradník (1991) to treat multiple surface points. This approach is understandably giving much more information than a simple 1D model, however, it really does not have real 3D performance, hence 1D-pseudo-3D modeling. From now on, we will (for simplicity) address the 1D-pseudo-3D method also as '1D'.

Either, the 3D FD and the matrix method, use the excitation by 2 complementary, separately computed, vertically incident, planar S-waves with a pulse time history given in velocities. Thus once the input pulse is positive to the North and has only NS component non-zero, and then the input pulse is positive to the East and is non-zero at the EW component. Thanks to such a division we are able to convolve the complete responses per partes with NS and EW component of an input seismogram. Adding the results then gives us an equivalent of long 2-component excitation while reasonably reducing the computational needs thanks to the fact, that a pulse response is, in principle, of a much shorter length. The 1-sided pulse in velocities has the integral normalized to 1:

$$f(t)=(4/(3*t))*((0.75-\cos(2*\pi*t/T))+.25*\cos(2*\pi*t/T)), \quad (2)$$

where  $PI=3.14159$ ,  $t$  is time, and  $T$  is a time constant given by the highest frequency ( $f_{hi}$ ) that corresponds to 1% of the spectral maximum of this function; that is here  $T=3.1/f_{hi}$ . The highest frequency for our computations is  $f_{hi}=12$  Hz. For later 3D and 1D computations, the lowermost layer corresponds exactly to the lowermost layer in models for the wave propagation. In that layer (regardless of time delay) we perform the S-wave injection/excitation.

After the pulse responses for whole  $195 \times 213$  points surface are computed, they have the same formal shape, regardless of the method (3D or “locally 1D”). We then convolved the EW and NS pulse responses in each point with the EW and NS components of a given seismogram, respectively, added the responses up and retrieved the complete 3D or 1D ground motion history. All the same was done for the reference models and respective method.

## COMPUTATIONS

### Input signals

For main tests we used the synthetic seismograms modelled by the PEXT method (Zahradnik, and Tselentis, 2002) computed for the Mw-5.9, 1999 Athens-like earthquake finite-extent source in  $\sim 10$  km distance (Oprsal et al., 2004, Oprsal et al, 2005). The reason for using synthetics is that it is relatively easy to compute pure incoming wave field without surface-reflected/refracted part. Further 20 ESMD (Ambraseys et al, 2002) recording were used and analysed. Nonetheless, the difference between synthetic and recorded signals responses was not reasonably different. The examples of the Athens-like 1999 and ESMD seismograms are shown in Figure 3.

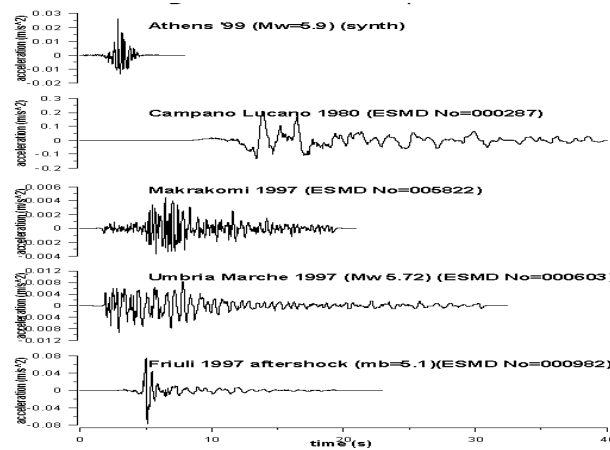


**Figure 3. Examples of several NS-component accelerograms used in the analyses.**

Analyses performed for multiple seismograms used two main groups

- 20 surface ground motions chosen from the CD2 of ESMD (Ambraseys, 2002). The choice of the data had several (not quite strict) criteria: A-rating category, solid rock or limestone, Mw  $\sim 4.3$ -6.5, and epicentral distance up to 50 km. A problem, while using this database, was sometimes a failure to display appropriate station information, while later trials for the same station showed different description/classification from ‘solid’ rock to ‘weathered rock’, etc (e.g., station Borgo-Cerreto Torre – record 000764). Following is the list of the records (accelerations, later integrated to velocities) used: 000055, 000059, 000140, 000242, 000287, 000359, 000363, 000365, 000382, 000384, 000597, 000598, 000603, 000604, 000621, 000706, 000764, 000981, 000982, 005822. Figure 3 shows example of the NS component of records Campano Lucano 1980 (ESMD No=000287), Makrakomi 1997 (ESMD No=005822), Umbria Marche 1997 (Mw 5.72) (ESMD No=000603), and Friuli 1997 aftershock (mb=5.1)(ESMD No=000982).
- 512 synthetic seismograms computed by modal summation (Fäh et al., 2006) for sources of varying depth, distance, orientation, and mechanism. The set is exactly the same as

in Fäh et al. (2006). The resulting synthetics are treated exactly in the same way as for the Athens-like earthquake or the ESMD ones, in terms of the convolution. Formally, the ‘radial’ component is taken for NS and ‘SH’ component as EW for all 512 seismograms.

### Response computations

#### *Athens-like 1999 earthquake, model [1,2]*

The main interest of the research was to investigate the earthquake ground motions and spectra amplifications in the Upper city to try to verify the hypothesis of an earthquake striking the city in ~250 A.D. We chose the  $M_w=5.9$  1999 Athens-like earthquake synthetics and the most favourable [gravel, Keuper] model [1,2] and the standard reference model Bedrock Swiss 1 to compute the spectral amplifications. Figure 4 shows a strong correlation between high PGV and PGA with topography. Moreover the topography in the Upper city of Augusta Raurica means mainly isolated hills consisting of gravels. The spectral amplification is depicted in left panel of Figure 5 shows. Very clear spots of high spectral amplifications reaching the value 9.1 are more all over the figure. The high-amplification regions are also very much isolated in space, and their typical size is about 100m. Comparing the PGA with PSA amplifications qualitatively, the PSA is clearly more scattered in space. For instance at the northern bank of the Violenbach river, or right north of the Upper city, the PGA maps do not show any reasonable amplitudes while the PSA amplifications are reaching values 5 and larger. As to the frequency content of the amplification, it is strongest at 4-6 Hz frequency band, and the amplification pattern is slightly more scattered for higher frequencies (right panel of Figure 5). Generally the large-amplification spots are up to 1.5 times larger in their maxima than in the mean value over a respective frequency band.

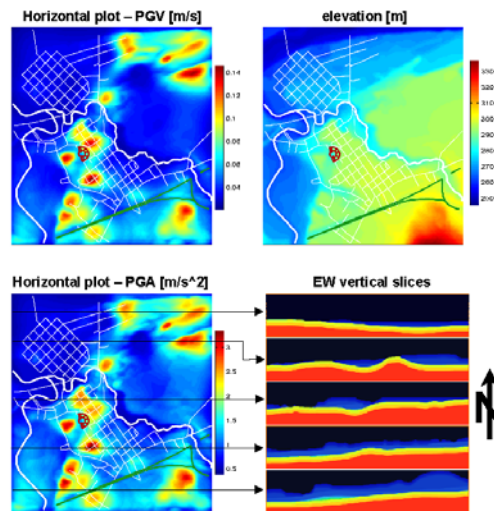


**Figure 4. Correlation between the topography combined with sediments and high PGA/PGV (left panels) for  $M_w=5.9$  1999 Athens-like earthquake in Augusta Raurica. Black arrows connect the surface traces of the vertical geology slices, vacuum shown as black colour, and PGA map. The thin white lines are historically re-mapped streets of the upper and lower city, Thick white lines are rivers Ergolz (left) and Violenbach (right). Red semi-ring denotes the amphitheatre, and the green lines in the southern part are for present-time highway. For more details see left panel of Figure 6.**

Difference of the PSA and PGA sensitivities to topography combined with underlying structure is distinctly demonstrated on the highway trace visible in the southern part of the PSA panels and very vague to none appearance of the same feature at PGA. At the same time, the riverbeds are well apparent on both PGA and PSAA.



### Correlation PSA vs collapsed structures

Historical findings of collapsed structures and remarkably buried human bodies represented by left panel of Figure 6 (for more details see Fäh et al. 2006) are generally well correlated with high PSAA of typical value between 5 and 8.

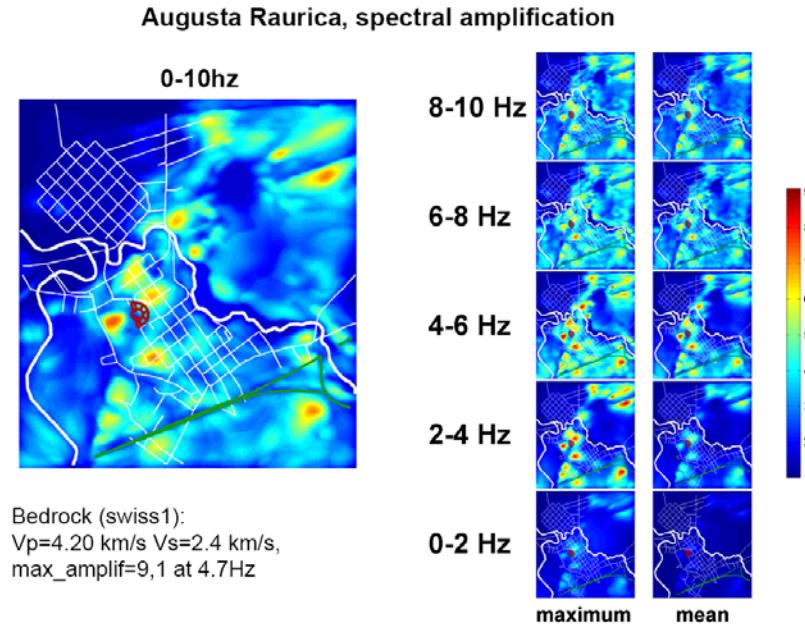


**Figure 5. (Pseudo) spectral amplification PSAA in the city area for 0-10 Hz, model [1,2], reference model bedrock Swiss 1 and M=5.9 1999 Athens-like earthquake. Decomposition into frequency bands in the right panel means ‘maximum’ and ‘mean’ values reached in each of the bands.**

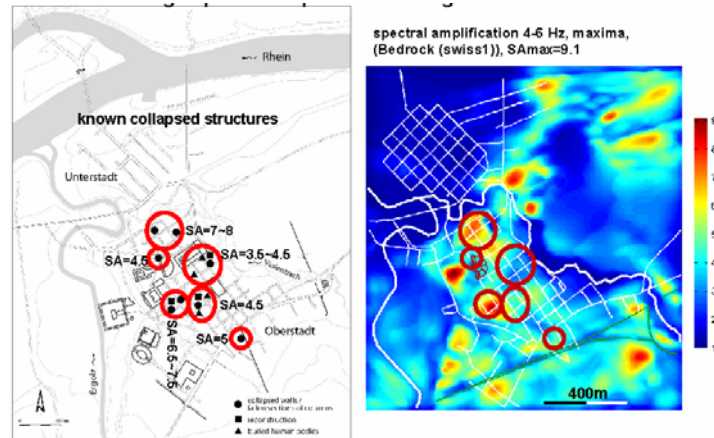


**Figure 6. Historical findings of collapsed structures and high spectral amplification (PSAA or SA) – red circles. Left panel is modified after Fäh et al. (2006), right panel are 4-6 Hz maximum values of the PSAA (M=5.9) taken from Figure 5. The numbers associated with the circles are approximate PSAA values in the circles.**

### Verifying upper-geology models

Favoured [1,2] model that we chose for our further investigations was not definitely very much distinct from the other three candidates. To conduct a reasonable comparison, we made the comparison between PSAA for various [gravel, Keuper] combinations by ratio of  $PSAA([1,2])/PSAA([gravel, Keuper])$  for each surface point separately. It's value is between ~ 0.95-1.81 and it shows the differences between the solutions for various models and our preferred [1,2] model (Figure 7a). The maximum values are 1.81 for [1,2] vs. [1,1] at 6-8 Hz, 1.68 for [1,2] vs. [2,1] at 0-2 Hz, and 1.39 for [1,2] vs. [2,2] at 8-10 Hz. Decomposed into 5 frequency bands, the main



difference appears in the southern part for 0-4 Hz and travels to the east and west for higher frequencies. From the similar behaviour of [1,2] vs. [1,1] and [2,1], and small values of [1,2] vs. [2,2] we deduce that the Keuper=2 model is responsible for higher amplifications and that the influence of the Keuper formation dominates over the influence of the gravels in term of combined gravel-Keuper effects.

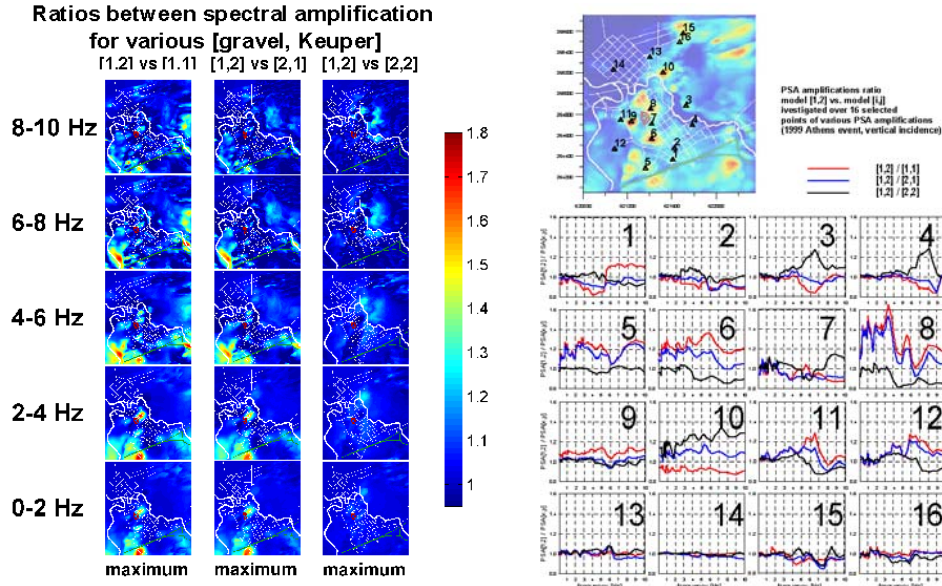


**Figure 7. a) Left- Maximum PSAA ratios (in each of the frequency band) for various top-geology models (Table 1) in Augusta Raurica, b) Right- Sensitivity of the PSAA to the top-geology models at 16 significant points (triangles). , (M=5.9, Athens-like earthquake)**

An insight into the sensitivity is given by examining the above [1,2] vs. [i,j] models at 16 significant points (chosen also for analysis, Fäh et al. 2006) depicted in Figure 7b. There is very small difference in point 13,14,15, and 16 being at the Northern part of the area. Point 1,2,3, and 4 situated east of the Upper city have typically less than 10% difference, except of 3 and 4 where [1,2] vs. [2,2] at 6.5 Hz and 8 Hz, respectively.

The above-mentioned similarity between [1,1] and [2,1] is represented by similar values for blue and red curves, differing by ~15% only in point 6 and 10, or being parallel to one another. The similarity between [1,2] and [2,2] is, on the other hand, represented by the black curve close to 1 or being approximately horizontal. The latter feature in similarities means similar pattern of the PSAA but not necessarily similar values. Points of stronger amplification are 5,6,8,9, and 10: 5 and 8 have very similar [1,1] and [2,1], being much weaker than [1,2]; point 10 has smallest PSAA for [2,2] model, and point 9 (largest PSAA=9.1 for bedrock Swiss 1) has very close values of PSAA for all 4 top-geology models. Point 9 correspond to an isolated hill where probably the geometrical features in wave propagation dominate regardless of the given material properties.

### Relevancy of reference models

A typical problem of less known structure in the field measurements is the reference-bedrock model. The sensitivity test is performed for model [1,2] and the 1999 Athens-like earthquake. Reference models Bedrock Swiss 1 and Bedrock Swiss 2 are tested against [1,2] models underlain by Bedrock Swiss 1 3D Top\_keuper-shaped structure; Bedrock Swiss 2 HI and Bedrock Swiss 2 LO are tested against Bedrock Swiss 2 HI and Bedrock Swiss 2 LO structures underlying the [1,2], correspondingly. The simplest reference model and corresponding bedrock model (Figure 1) is Bedrock Swiss 1 (Table 2) is considered our generic model. PSAA pattern for Bedrock Swiss 1 and Bedrock Swiss 2 cases do not practically differ in the shape of the PSAA pattern (Figures 5, and 8, mid panel), and the frequency band of largest amplification, while the maximum PSAA for Bedrock Swiss 2 is only 20% higher than for Bedrock Swiss 1. On the other hand, comparing Bedrock Swiss 2, Bedrock Swiss 2 LO and

Bedrock Swiss 2 HI in Figure 8 is more interesting because the large-amplification spots equalize in terms of PSAA amplitude. It happens mainly thanks to a migration of higher PSAA to the East and to their slight overall increase (with max PSAA = 9.2 for Bedrock Swiss 2 HI). Last but not least, the lower frequency of the highest PSAA dropping from steady 5.7 Hz to 3.8 Hz corresponding to thicker gravel layer (see EW slices in Figure 4, right-lower panel). Probably, the wave field is more prone to create standing waves at these parts of the model for higher bedrock velocities. Localized topography edge effects belonging to non-isolated topography structures (like end of plateau or flat topography ridge) are modelled only by 3D method, hence strong 3D/1D values.

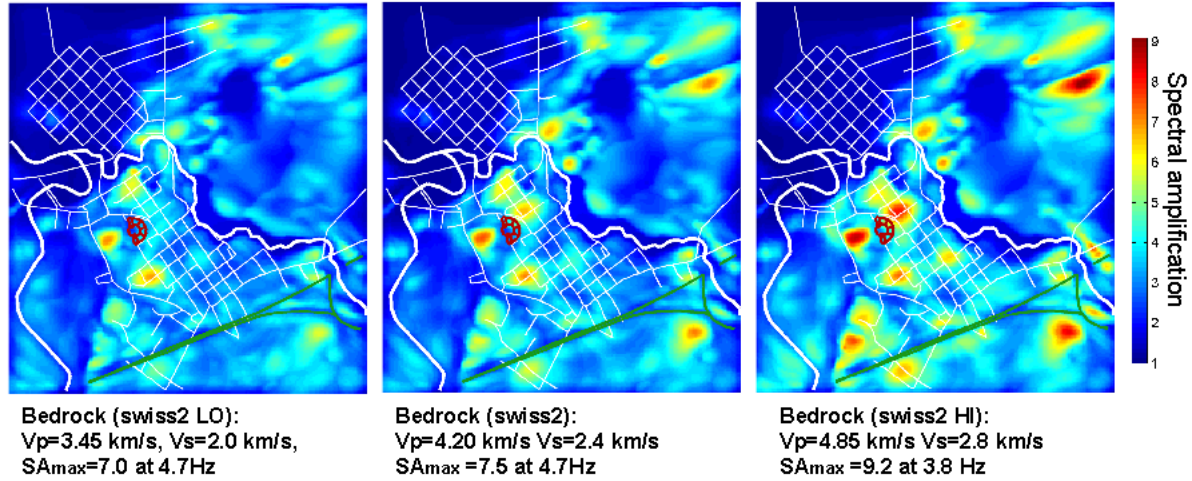


**Figure 8. Sensitivity of the PSAA to 3 alternative bedrock models (Table 2), M=5.9 Athens-like earthquake, top geology model=[1,2] (Table 1).**

### 3D vs 1D modelling

Other interesting result is aiming at the importance of full 3D modelling by the difference between “locally 1D” and 3D computations. In this case (still for the Athens-like 1999 earthquake) the ratio  $PSAA(3DFD, \text{model}[1,2])/PSAA(\text{“locally 1D”, model}[1,2])$  is evaluated. Figure 9 shows that a difference between the amplifications evaluated for each of the methods is expressed by the ration of 4.3 (at 4.2 Hz) in the magnitude of amplifications. In the Upper city it still reaches 2.9. Such a ratio is not evenly distributed, but is often localized in spots with high PSAA (e.g., points 6, 8, 9 of Figure 7b). Generally high 3D/1D PSAA appears due to topography of solid hill or ridge-like and of topography plateau that create wave propagation effects unknown to 1D methods. The pronounced PSAA in the 3D FD case is not only due to the presence of the Keuper layer, but due to it’s combination with pronounced topography. Decomposed into frequency bands, higher 3D/1D is more scattered at higher frequencies and correlates with topography edges (rightmost panel of Figure 9).

### 3D, 1D and 3D vs 1D for 3 areas

Detailed geophysical and geological investigations and measurements of fundamental frequencies demanded the division of the city into 5 zones and their subzones (totally 8 areas), each being consistent in terms of similar geology and shape of the H/V spectral ratios (Ripperger, Fig. 2, 2002, Fäh et al., 2006, Fig. 5).

From the PSAA and 3D/1D PSAA ratios were for the 8 areas (sub-zones) we display here results for zone IIa,b (Upper city – Oberstadt) and IV (Lower city – Unterstadt) (Figure 10). Number of the investigated surface points in IIa,b, and IV is: pts(IIa)=3109, pts(IIb)=519, pts(IV)=2036. Because of the pronounced amplitudes of resulting wave field from the 3D FD modelling we modified the ESE border of zone IV To exclude surface point with systematically different amplification characteristics. For each of the sub-zones, the statistical values over all points in a respective sub-zone were computed. 3D PSAA in zone IIa and Iib have maxima a way above the mean. This indicates very localised high-PSAA regions inside the sub-zones. The maximum PSA amplification is above 8 for frequencies around 5 Hz, and average values are typically 3.5-4 for 3-10 Hz. 1D PSAA is ~1 up to 3

Hz, and rises up to 3-4 above 4 Hz in IIa and IIb for either envelopes and maxima. It indicates low localizing of the site effects. Both 3D and 1D PSAA are very quiet in zone IV with PSAA~1-1.5 up to 4Hz and maxima reaching 2.5 at 10 Hz. The mean of 3D/1D PSAA is ~1 for all frequencies and all zones, the envelope of 3D/1D PSAA reaches 2.7 at 4.5 Hz (IIa) and 2.3 at 7.5 Hz (IIb). Typical value is over 1.5 for envelopes in IIa,b.

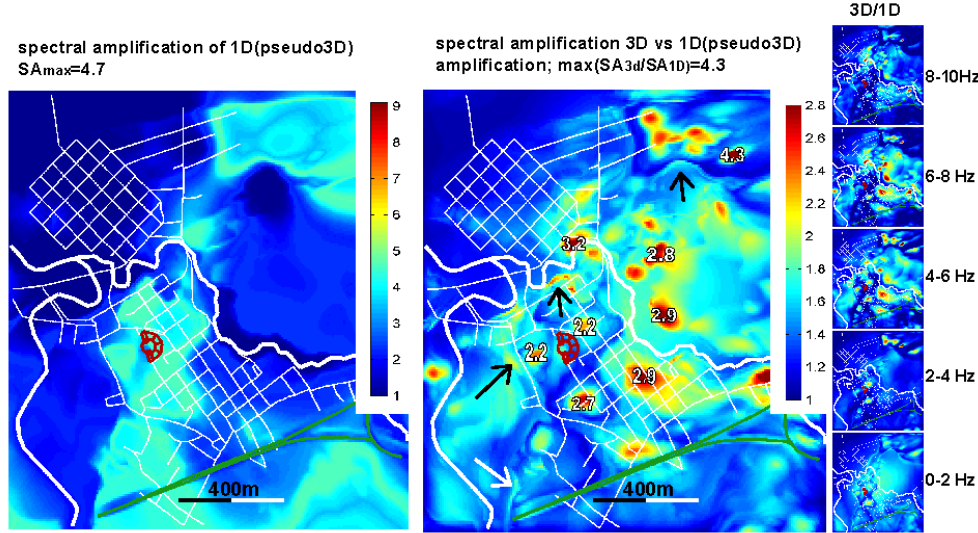


**Figure 9. 1D vs. 3D spectral amplification. “Locally 1D” (left) is compared with full 3D FD modelling (Figure 5). Numbers (right) denote the PSAA of 3D/1D values, arrows point to several localized topography edge effects (like end of plateau)**

Statistical investigation of the 3D/1D behaviour was studied by an analysis of PSAA(3D)/PSAA(“locally 1D”) for 20 signals from the European Strong Motion Database (Ambraseys et al. 2002) and 5 zones as described above. In Figure 10 is a comparison for zones IIa,b and IV in statistical values of mean, standard deviation, and envelopes of 1D and 3D PSAA, and 3D/“locally 1D” PSAA ratio performed over all points in the respective (sub)zone and over all 20 records. The features of the envelopes are similar to those of 1999 Athens-like earthquake, but at the same time, the mean values are much smoother. Standard deviation is typically 25% of respective mean value. The maximum 3D/1D ratio in IIa exceeds 3 at 5 Hz.

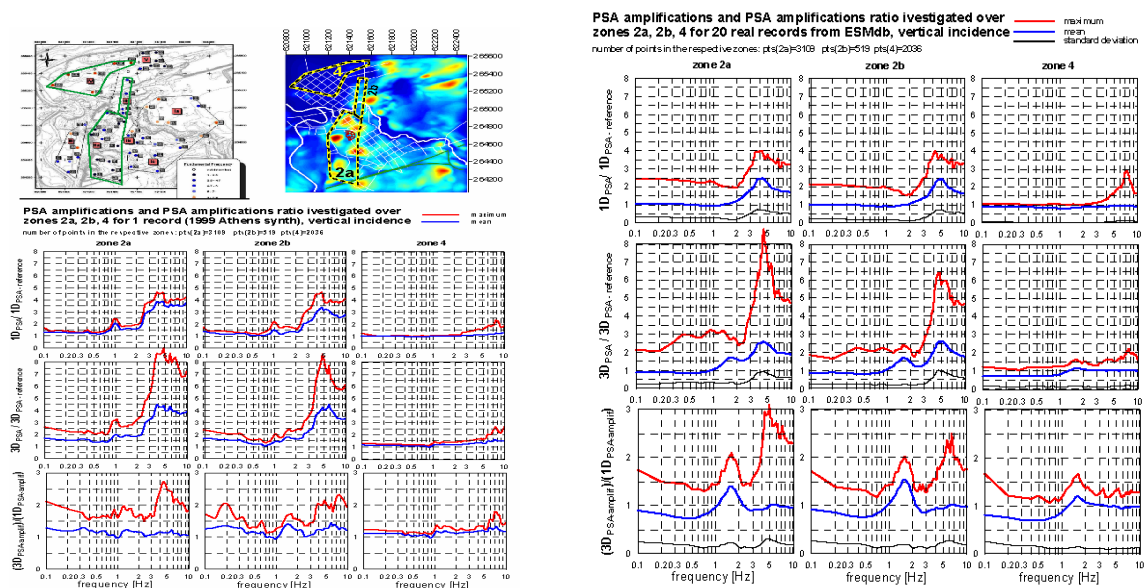


**Figure 10. PSA amplifications and PSA amplifications ratio**

## CONCLUSIONS

We investigated the earthquake ground motion features in the historical archaeology site of Augusta raurica city in terms of PGA, PGV and pseudospectral amplification for  $m=5.9$  1999 Athens-like earthquake, and 20 European strong motion database records for 0-10Hz band. Four various combinations of [gravel, Keuper] surface geology, 4 bedrock structures, and interface shape between them were tested against H/V data – relative difference to data is typically up to 15%. Sensitivity to lower-based Keuper layers' variations seems to be higher than that to gravel lying on the top. Measured by PSAA against most favoured [1,2] [gravel, Keuper] model, the amplitudes differ typically (–10 ... +20)% in the area of interest. As to the bedrock, the sensitivity to lower values seems to be minor to higher values of the S-wave velocities ( $V_s$ ). Higher  $V_s$  in the bedrock also changes the shape of the PSAA pattern in terms of their relative amplitudes. Topography and topography edge effects are visible PGA maps as well as in the PSAA plots, however, the PSAA seems to show generally more details at spots of topographic graves. Amplitudes of PSAA reach maxima of 6 - 9.1 for chosen geology model. The Upper city area, and it correlates (by  $PSAA > 5$ , typically) with known collapsed structures in the Upper city. We demonstrated the importance of 3D wave field propagation modelling in the top 40 m of the structure. The ratio of PSAA between commonly used 1D and our full-wave filed 3D modelling (show are 0-10Hz results) is reaching 3 between 3.5-7.5 Hz in the upper city, and spots of such differences are relatively local in space. So far, the correlation of high PSAA and archaeological findings are the only serious candidates to support the 250AD earthquake striking the city

## ACKNOWLEDGEMENTS

This research has been funded by the Swiss National Science Foundation (Nr. 1214-63542.00; Nr. 100012-105352), and supported by the EU project SPICE (MRTN-CT-2003-504267); this presentation is supported by Japanese Society for Promotion of Science award FY2006/P06320.

## REFERENCES

- Ambraseys et al., ESMD - European Strong Motion Database, CD2, 2002.
- Bartak, V., Zahradnik, J., Program SITEF\_MULT, version 1991, modified by Oprsal, I. for code sitefio.f90, 2004.
- Fäh, D., Steimen, S., Oprsal, I., Ripperger, J., Wössner, J., Schatzmann, R., Kästli, P., Spottke, I., and Huggenberger, P., The earthquake of 250 A.D. in Augusta Raurica, A real event with a 3D site-effect? *Journal of Seismology*, DOI:10.1007/s10950-006-9031-1, 19pp, 2006.
- Kind, F., Development of microzonation methods: Application to Basel, Switzerland, Ph.D. thesis 14548, ETH Zurich, Zurich, Switzerland, 2002.
- Mueller, G., The reflectivity method: a tutorial. *J. Geophys.*, 58, 153-174, 1985.
- Opršal, I., Brokešová, J., Fäh, D., and Giardini, D., 3D Hybrid Ray-FD and DWN-FD Seismic Modeling For Simple Models Containing Complex Local Structures, *Stud. Geophys. Geod.* 46, 711-730, 2002.
- Opršal, I.; Fäh, Donat; Mai, and P. Martin; Giardini, D., Deterministic earthquake scenario for the Basel area: Simulating strong motions and site effects for Basel, Switzerland, *J. Geophys. Res.*, Vol. 110, No. B4, B04305, DOI:10.1029/2004JB003188, 2005.
- Oprsal, I., Zahradnik, J., Three-dimensional finite difference method and hybrid modeling of earthquake ground motion, *J. Geophys. Res.*, 107(B8), DOI 10.1029/2000JB000082, 16pp, 2002.
- Opršal, I., Zahradnik, J., Serpetsidaki, A., and Tselenits, G.-A., 2004. 3D hybrid simulation of the source and site effects during the 1999 Athens earthquake. *Proc. of 13th World Conference on Earthquake Engineering*, Vancouver, B.C., Canada, August 1-6, 2004, Paper No. 3337, 15 pp.
- Ripperger, J., Records of earthquakes, battles, and reconstructions in Augusta Raurica: an archaeological and seismological research project, Second Report: June 2003.
- Zahradnik, J., and G.-A. Tselentis, Modeling strong-motion accelerograms by PEXT method, application to the Athens 1999 earthquake, in *Proceedings of XXVIII General Assembly*, 1 – 6 Sept. 2002, Genoa [CD-ROM], Eur. Seismol. Comm., Edinburgh. (available at <http://seis30.karlov.mff.cuni.cz/>)
- Zahradnik, J., Jech, J., and Moczo, P., Absorption correction for computations of a seismic ground response, *Bull. Seismol. Soc. Am.* 80, 1382– 1387, 1990a.
- Zahradnik, J., Jech, J., and Moczo, P., Approximate absorption corrections for complete SH seismograms, *Stud. Geophys. Geod.*, 34, 185– 196, 1990b.